

On the Randomness of Natural Fractures

Eric B. Niven and Clayton V. Deutsch

Discrete Fracture Networks (DFNs) are commonly generated using random fracture locations and orientations selected randomly from an input distribution. This results in artifacts such as unrealistic fracture spacing or orientation compared to fractures observed in nature as well as fractures from the same set crossing at low angles. Two real-life fracture networks are examined in more detail. The first is a photo of fractures exposed in a rock cut. The second is a map of fractures measured from an outcrop in Northern Alberta. These two measured fracture networks are compared to multiple realizations of DFNs created using random fracture locations and orientations. It is shown that the DFNs utilizing random fracture locations and orientations are unable to accurately model the fracture spacing, inter-fracture orientation and number of fracture intersections seen in the measured fracture networks.

1. Introduction

Observations indicate that it is possible to describe fracture attributes with a variety of statistical distributions. Joint length and aperture are often interpreted to follow a log-normal distribution. Other studies suggest that fault systems have attributes that follow a power-law or fractal distribution.

Unfortunately attempts to analyze the spatial distribution of fracture systems have been less successful. Typical DFN generation schemes rely on distributing the fractures in space with a Poisson process with fractures that are independent and lack spatial correlation (Gauthier et al. 2002, Hitchmough et al. 2007). This may lead to negative exponential spacing distributions and fails to account for the clustering of joints (Belfield 1998). However, some research has indicated the fracture spacing is log-normally distributed (Narr et al. 2006), indicating that fractures are not distributed independently. Despite this, the use of Poisson models to generate fractures persists.

When DFNs are generated with random locations and an input orientation distribution, the models typically contain two undesirable features. First, due to the nature of generating random locations, it is possible to generate fractures that are extremely close together or far apart. As a result, most DFNs do not respect the fracture spacing seen in nature. Second, if the fracture orientation distribution is wide enough, fractures from the same set may cross each other at low angles.

Fractures do not occur randomly in space. Rather, they are created when the stress in intact rock exceeds its strength. When a fracture is created, the stress in the surrounding rock is reduced. Thus, it becomes very rare for a new fracture to form close to one that has recently been created. With a random fracture seed location when generating the DFN, fractures can be created that are unrealistically close or far.

Another artifact of DFNs generated with random fracture locations and orientations is fractures from the same set which cross each other at low angles. This is rare in nature, except in the case of en-echelon fractures. Figure 1 shows an example of the artifacts that may show up in a DFN with random fracture locations and randomly sampled fracture orientations. Note that the fractures in Figure 1 are meant to simulate only 1 fracture set.

This paper examines images of fracture patterns seen in nature and attempts to determine whether or not those fracture patterns could be recreated by a DFN algorithm that generates fracture location and orientation randomly.

This paper is part of a series of four articles in this report that pertain to fracture modeling. This paper discusses and presents evidence that some natural fracture networks cannot be accurately modeled using traditionally created DFNs. Niven and Deutsch (2010a) present the new approach to modeling DFNs. Niven and Deutsch (2010c) present a new computer program to simulate DFNs using the methodology described in this paper. In Niven and Deutsch (2010b) a real-life example is presented. DFNSIM is used to model measured surface lineaments from Northern Alberta. The modeling process is discussed in detail.

2. The Distribution of Fracture Spacing from Randomly Located Fractures

A simple two-dimensional DFN was constructed where the fracture locations were generated randomly. The DFN is shown in Figure 2. As can be seen in the figure, there are places where fractures are unrealistically close to each other, there are fractures that cross at low angles and there are large areas without fractures.

Next, the fracture spacing distribution for the DFN was calculated using a program called CALCSPACING. The program draws an imaginary scan line through the DFN that is perpendicular to the average fracture orientation. The program then notes the locations where the scan line intersects a fracture. Then, the distances between the intersection points (the fracture spacing) are calculated and recorded. The program repeats this process with many scan lines until a stable distribution of fracture spacing is calculated.

For the DFN shown in Figure 2, the distribution of fracture spacing (Figure 3) corresponds to a lognormal distribution using the fracture spacing mean and standard deviation. It is often noted in the literature that fracture spacing follows a lognormal distribution (Belfield 1998), although as the figure shows, this is not quite true for a randomly generated DFN.

3. Case 1: Digitized Photo of a Rock Cut

Figure 4 shows an exposed rock face along a walking trail near Vernazza, Italy, taken by the first author. The rock face shows two fracture sets. There are three well defined fractures that are easily identified, which dip towards the lower left corner of the photo. The other fracture set has many more fractures that are less defined and dip toward the lower right corner of the photo.

The traces from the second fracture set were digitized. The digitized fracture traces are shown in Figure 4. In total, 48 fractures from that fracture set were digitized.

To keep things simple, assume that:

- The digitized fractures in Figure 4 are two-dimensional
- That Figure 4 shows them in plan view (i.e. from overhead), since their actual orientation is unknown and the photo is taken at an oblique angle to the rock face.
- That North points up in Figure 4.

With these assumptions in mind, the average fracture orientation (defined by the trend of the fracture) is 71.7 degrees clockwise from north with a standard deviation of 7.1 degrees. The distribution of fracture orientation is approximately normal.

Figure 5 shows a histogram of fracture spacing for the digitized fractures from the photograph (shown in Figure 4). As there is no accurate distance scale for the photograph, distance is measured in pixels. Figure 5 also shows the histogram of fracture spacing if the same fractures (i.e. same length) are generated by a DFN that assumes randomly located fractures and orientations drawn from a normal distribution with mean and standard deviation of 71.7 and 7.1 degrees, respectively. Note that the histogram shown for the randomly relocated and re-oriented case is for 100 realizations. Multiple realizations were used in order to obtain a smooth histogram. Figure 5 shows that the rock face fractures are not spaced the same as the randomly located fractures. The rock face fracture histogram shows a greater incidence of fracture spacing below 400 pixels and a lower incidence of fracture spacing above 400 pixels.

Figure 5 shows histograms of inter-fracture angle for 1) the original rock face fractures shown in Figure 4 and for 100 realizations of randomly relocated and re-oriented fractures. The histogram for the digitized fractures shows a much higher incidence of low inter-fracture angle than for the random case. This means that fractures that are close in the digitized image are likely to be oriented more similarly than they would be if they were randomly oriented.

In addition to fracture spacing and inter-fracture orientation, the number of fracture intersections was calculated for the digitized fracture data as well as the randomly relocated and re-oriented fracture data. It turns out that there are no fracture intersections in the digitized fracture data. This is easily seen by examining the data visually in Figure 4. However, in the randomly relocated and re-oriented fracture networks, fracture intersections are quite common. A histogram of the number of

fracture intersections in the randomly relocated and re-oriented fractures is shown in Figure 6. In 100 realizations of relocated and re-oriented fracture networks there is an average of 3.9 fracture intersections with a standard deviation of 2.1 intersections. Furthermore, out of the 100 realizations there were only two realizations that showed no fracture intersections.

Taken together, the fracture spacing, inter-fracture angle and fracture intersection data indicate that the fractures shown on the rock face in Italy could not be modeled with a naïve DFN that generates fractures randomly with a Poisson process.

4. Case 2: Fracture Map

Figure 7 shows a map of two fracture sets trending southwest-northeast and southeast-northwest in an area of Northern Alberta (Pana and Waters 2001). The southwest-northeast fracture set was digitized for further analysis. In total, there are 425 fractures from the SW-NE fracture set (Figure 7). Figure 8 and Figure 9 show a contoured stereonet and a rose diagram of the fractures, respectively. Although the stereonet and the rose diagrams indicate that the fractures are from a single set, from a qualitative standpoint there appears to be some pattern to the fracture locations and orientations. Namely, there are few fractures that intersect and fractures appear to be oriented similarly to their nearest neighbors.

Figure 10 shows the histogram of fracture spacing for the fracture data (in Figure 7). The spacing if the fractures are randomly relocated and re-oriented is shown on the same figure. For the random scenario, 30 realizations were generated and used to calculate a stable and smooth fracture spacing distribution. Here, fewer realizations were required to achieve a stable distribution since there are more fractures than in the first example.

The spacing calculations reveal that the fractures in Figure 7 have an average spacing of 17.7 km and a standard deviation of 17.4 km. The randomly located fractures have a larger average spacing and standard deviation of 24.1 and 23.4 km, respectively. Moreover, the fracture spacing distribution for the real data is narrower and less more positively skewed. Note that the distribution peaks at a fracture spacing of approximately 13 m compared to the random case which peak in the first bin (approximately 3 m). The real fractures (Figure 7) display a more regular spacing pattern (lower standard deviation) than the random fractures. This suggests that a DFN created using randomly located fractures is not able to respect the correct fracture spacing distribution.

To determine if the two distributions are the same a Kolmogorov-Smirnov test was applied. The test statistic, D , is the absolute maximum difference between the two distributions. In this case, the D -statistic is 0.186. Using a significance level of 0.01, the corresponding critical value of the D -statistic is 0.030. Since the value of the calculated D -statistic is well above the critical value we reject the hypothesis that the two distributions are the same.

Next, the difference in orientation between each fracture in the data set and its nearest neighbor was determined. Figure 10 also shows the histogram of inter-fracture angle for the 30 realizations of randomly relocated and re-oriented fractures. In this case, the re-oriented fractures were generated by randomly selecting from a normal distribution with a mean and standard deviation of 146.5 and 11.8 degrees, respectively. The fractures from the true fracture data set (Figure 7) are oriented more similarly than the fractures in the DFN; in this case, the Kolmogorov-Smirnov D -statistic is 0.208. Using a significance level of 0.01, the corresponding critical value of the D -statistic is 0.0144 and the hypothesis that the two distributions are the same is rejected.

A program was constructed to calculate the number of fracture intersections in a DFN. In the map of fractures in Northern Alberta (Figure 7) there are 20 fracture intersections in the digitized fracture set. Next, the fracture intersections were calculated for each of the 30 DFNs with random fracture locations. The random realizations have 89.4 intersections on average with a standard deviation of 8.9 intersections. Thus, an average of 20 intersections as in the fracture map of Northern Alberta, is approximately 7.5 standard deviations away from the mean of the random location scenario.

Taken together, the fracture spacing, inter-fracture angle and fracture intersection data indicate that the fractures shown on the rock face in Italy could not be modeled with a naïve DFN that generates fractures randomly with a Poisson process.

5. Conclusions

Discrete fracture networks (DFNs) are commonly generated using a Poisson process to generate fracture locations and simulating fracture orientations drawn from an input distribution typically selected from the available fracture data. As a result many DFNs show unusual artifacts such as fractures that are spaced extremely close together or far apart, or fractures from the same set that intersect at low angles.

Two examples were presented in this paper. In the first, a rock cut was photographed and the observed fractures were digitized. In the second, a map of fractures in Northern Alberta was digitized. For both examples it was shown that DFNs generated using random fracture locations and orientations randomly selected from an input distribution are not able to match the fracture spacing, inter-fracture angle and number of fracture intersections seen in the measured fracture networks. In paper 102 (Niven and Deutsch 2010a) we present a methodology to explicitly honor these spatial features of fracture networks.

References

- Belfield, W.C. 1998. Incorporating spatial distribution into stochastic modelling of fractures: Multifractals and levy-stable statistics, *Journal of Structural Geology*, **20**(4): 473-486.
- Gauthier, B.D.M., Garcia, M., and Daniel, J.M. 2002. Integrated fractured reservoir characterization: A case study in a north africa field, *SPE Reservoir Evaluation & Engineering*, **SPE 79105**: 284-294.
- Hitchmough, A.M., Riley, M.S., Herbert, A.W., and Tellam, J.H. 2007. Estimating the hydraulic properties of the fracture network in a sandstone aquifer, *Journal of contaminant hydrology*, **93**(1-4): 38-57.
- Narr, W., Schechter, D.S., and Thompson, L.B. 2006. Naturally fractured reservoir characterization. Society of Petroleum Engineers, Richardson, Texas.
- Niven, E.B. and Deutsch, C.V. 2010a. A new approach to DFN simulation. Paper 102, Report 12, Centre for Computational Geostatistics, University of Alberta, Edmonton, Alberta.
- Niven, E.B. and Deutsch, C.V. 2010b. An example application of DFNSIM in modeling surface lineaments. Paper 206, Report 12, Centre for Computational Geostatistics, University of Alberta, Edmonton, Alberta.
- Niven, E.B. and Deutsch, C.V. 2010c. DFNSIM: A new program for simulating discrete fracture networks. Paper 402, Report 12, Centre for Computational Geostatistics, University of Alberta, Edmonton, Alberta.
- Pana, D.I. and Waters, J.:G., M. 2001. GIS compilation of structural elements in northern alberta, release 1.0. 2001-01, Alberta Energy and Utilities Board - Alberta Geological Survey, .

Figures

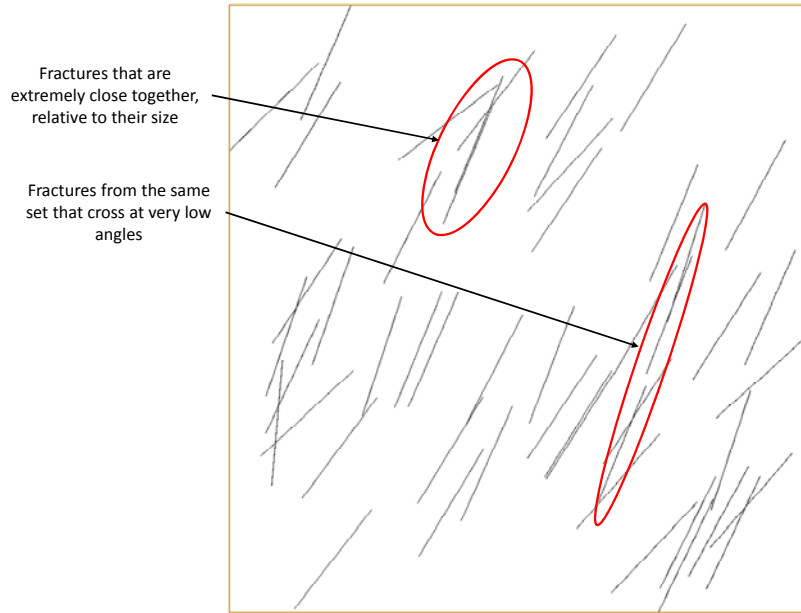


Figure 1: DFN created with random fracture locations and orientations drawn from an input distribution.

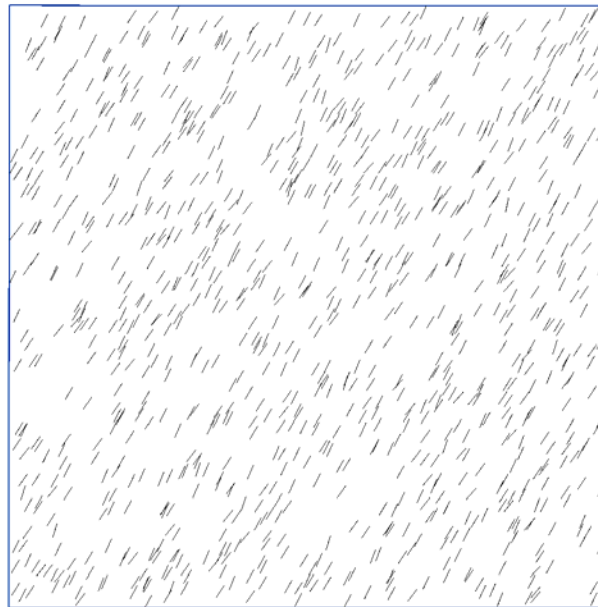


Figure 2: A DFN with 1000 fractures created using random fracture locations.

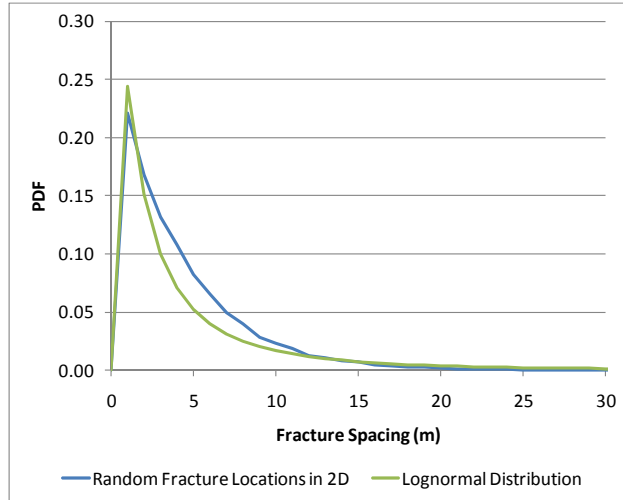


Figure 3: The fracture spacing distribution for the DFN along compared to its lognormal distribution.



Figure 4: On the left: An exposed rock face showing two fracture sets in Vernazza, Italy. On the right: One of the fracture sets is digitized.

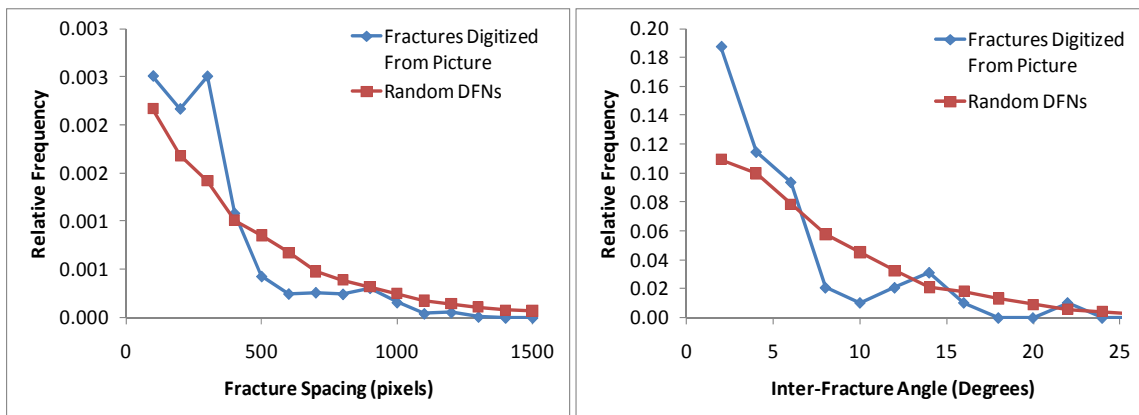


Figure 5: histograms of fracture spacing for the digitized fractures (Figure 4) and for 100 random realizations. The spacing is measured in units of pixels as there is no accurate scale for the photograph. On the right: histograms of inter-fracture angle for the digitized fractures (Figure 4) and for 100 random realizations.

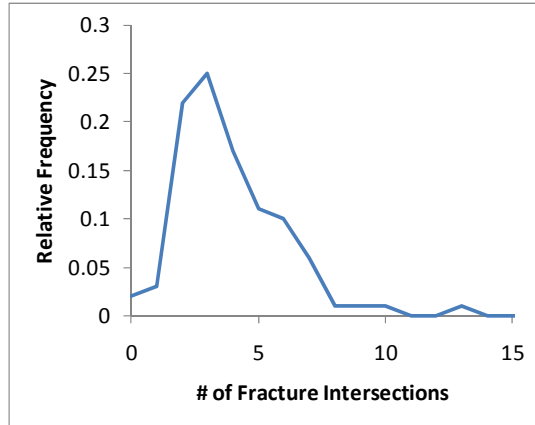


Figure 6: A histogram of the number of fracture intersections measured in 100 realizations of randomly relocated and re-oriented fractures.

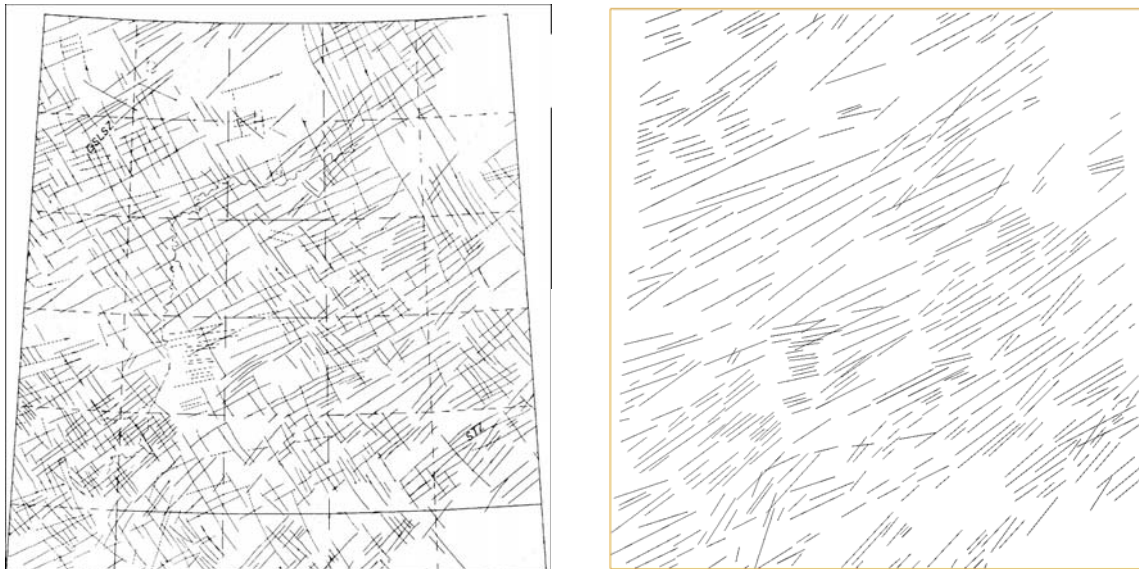


Figure 7: On the left: A map of fractures from Northern Alberta (Pana and Waters 2001). On the right: The southwest-northeast set digitized.

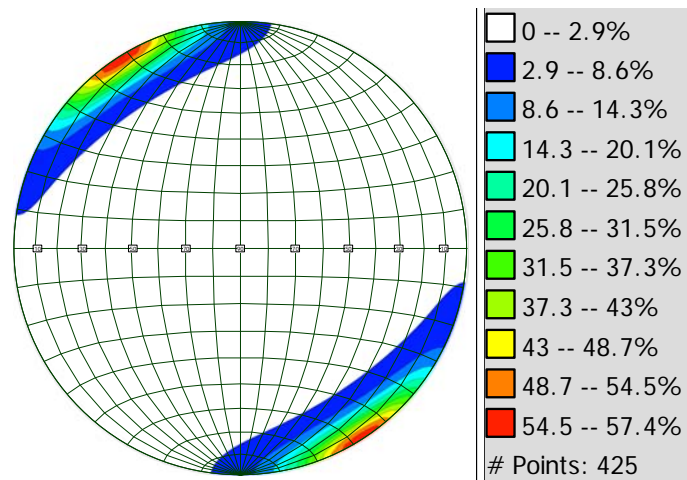


Figure 8: Schmidt equal area stereonet for the fractures shown in Figure 7.

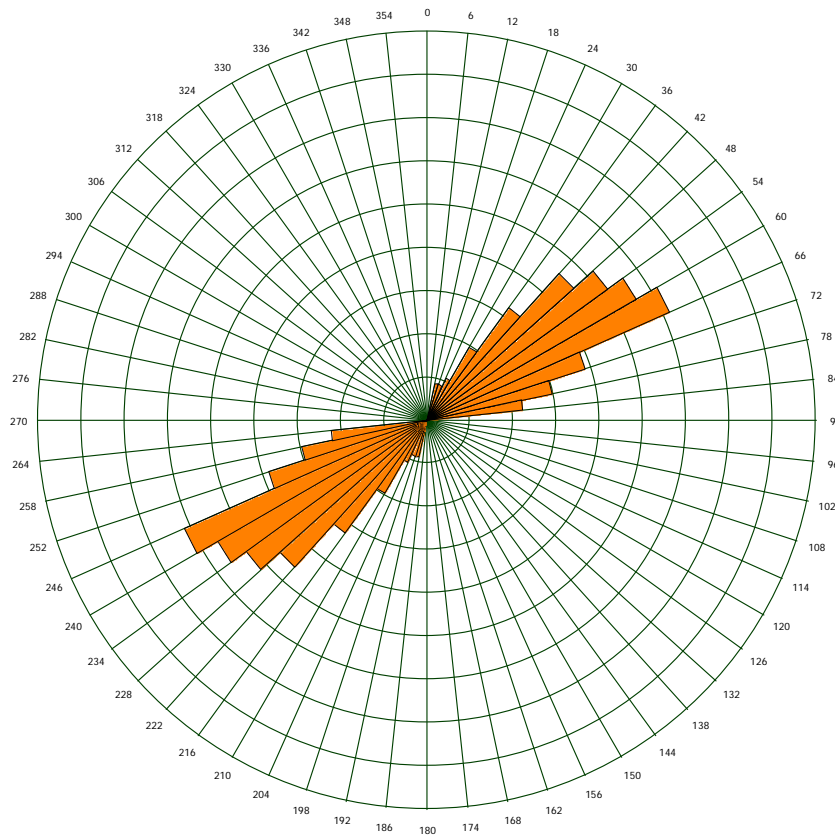


Figure 9: Rose diagram for the fractures shown in Figure 7.

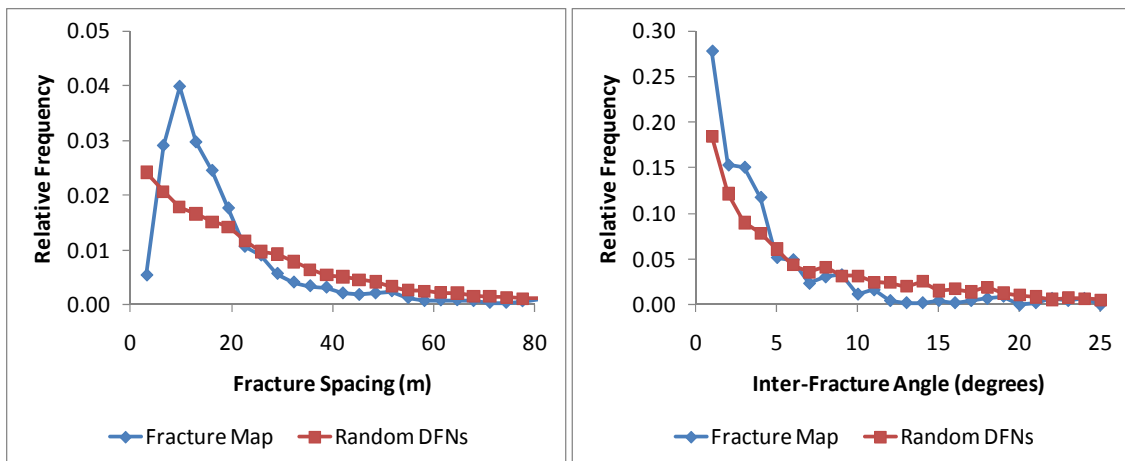


Figure 10: On the left: Fracture Spacing for the image shown in Figure 7 compared to 100 realizations of random fracture locations. On the right: The distribution of the angle between any fracture and its nearest neighbor for the image shown in Figure 7 and for the same fractures with partially random orientations.